Experimental study of the wind flow in a coastal region of Japan

Atsushi Yamaguchi*, Takeshi Ishihara, Yozo Fujino

Department of Civil Engineering, University of Tokyo, 7-3-1 Hongo Bunkyo, Tokyo 113-8656, Japan

Abstract

Wind flow over complex and steep terrain was investigated by a wind tunnel experiment and a numerical simulation. The mean value and the turbulence of the wind flow over complex terrain in a coastal region of Japan were measured by split-fiber and X-wire probes. It was found that the split-fiber probe can give a reasonable accuracy while the conventional X-wire probe measurement contains a large error because of the existence of reverse flow and strong across wind in complex terrain. The applicability of the power law to the wind prediction over complex terrain was also examined. It was noticed that the application of the power law for the estimation of the wind speed or the turbulence intensity in complex terrain is difficult. Numerical simulations were carried out by the non-linear model developed by the authors and the conventional linear model. The wind field predicted by the non-linear model shows fairly good agreement with the experiment while conventional linear model tends to overestimate the mean wind speed and underestimate the turbulence.
© 2002 Elsevier Science Ltd. All rights reserved.

Keywords: Wind tunnel study; Complex terrain; Split-fiber probe measurement; Numerical simulation

1. Introduction

Prediction of the turbulent flow over complex terrain plays a dominant role in engineering applications such as the efficient extraction of wind energy and the safety of structures. Numerical models are widely used for the prediction of the flow over terrain. For the flow over moderate terrain, governing equation can be linearized and the model proposed by Jackson and Hunt [1] is based on this idea. However, the linear model loses its prediction accuracy remarkably when the terrain is steep as seen in a coastal region of Japan.

---

*Corresponding author. Tel.: +81-3-5841-6099; fax: +81-3-5841-7454.
E-mail address: atsushi@bridge.t.u-tokyo.ac.jp (A. Yamaguchi).

Recently, non-linear models have been paid attention because the non-linear model does not linearize the governing equation and has no limitation on the slope angle. The earliest use of the non-linear model for the prediction of the wind flow over steep terrain is attempted by Coelho and Pereira [2]. Non-linear model was also used for the wind prediction over real complex terrain. Maurizi et al. [3] changed the mesh size from 200 to 500 m and investigated the mesh size dependencies of the predicted wind flow. They concluded that the prediction error in the coarse mesh is about 15%, but the numerical results were not verified by experiment. To examine the performance of numerical models, an accurate experimental data of the flow over complex terrain is needed, but no such data is available.

The objective of this study is to obtain high-quality data of the flow over complex terrain by a wind tunnel experiment and verify the performance of the numerical models for predicting wind flow in a coastal region of Japan. The mean flow and the turbulence over a real terrain were measured by X-wire and split-fiber probes. The errors in the X-wire measurements are investigated by comparing with the split-fiber measurement. Furthermore, the numerical simulations are carried out by the non-linear model developed by the authors and the conventional linear model and are compared with the measurements to verify the performance of these models.

2. Experimental setup

2.1. Facility and terrain model

The experiment was carried out in a circuit wind tunnel in the Wind Engineering Laboratory, the University of Tokyo, which has a working section of 16 m wide, 1.9 m high and 5.8 m long. A neutrally stratified atmospheric boundary layer was simulated using two 30 mm high cubic arrays placed just downstream of the contraction exit. The wind speed outside the boundary layer was monitored with a Pitot tube and maintained at 6.0 m/s throughout the experiment. The resulting boundary layer has a thickness of 150 mm at the measurement sites and has the scale of 1:2000.

A part of Shakotan Peninsula area, north of Japan, was chosen for the experiment. The topographic feature of the area is very complex with a steep cliff along the north-east coast. A 1:2000 scale terrain model with a diameter of 4 m was made, which covers an area of 8 km. The model was made from 5.5 mm thick plywood and covered with the mixture of glue and sand to represent the terrain surface covered with grass. The surface roughness length of the model is 0.01 mm which corresponds to 2 cm in the real scale. Fig. 1 shows the terrain model installed on a turn table. The flow measurements were performed in eight wind directions.

Fig. 2 shows the measurement locations and the elevation contours of the terrain model. Points A–G in the figure correspond to the observation masts described by NEDO [4]. Although all the sites are located on a plateau except for G, the surrounding terrains are quite different. Terrain around the mast A and E are relatively flat and less complex, while terrain around the mast B, C and D are very
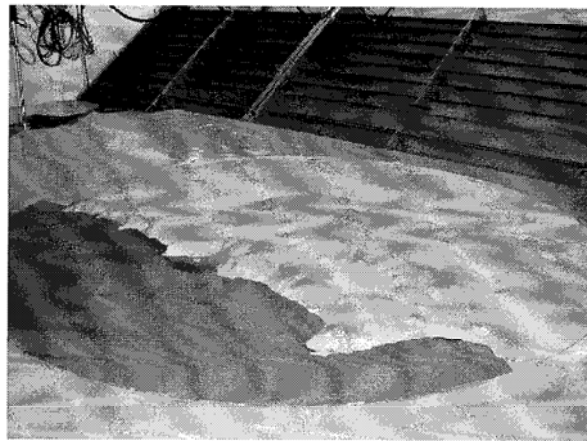
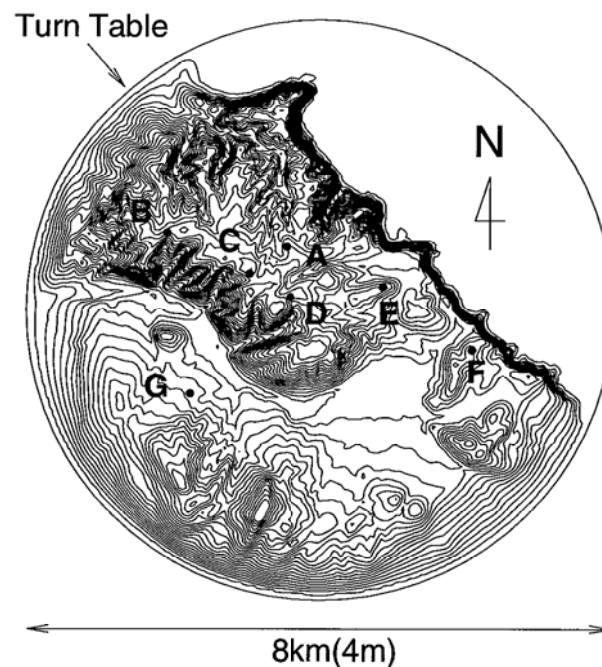Fig. 1. The wind tunnel and the terrain model.

Fig. 2. The elevation contour of the terrain model and the measurement sites.

complex. At the northeast side of the mast F, there is a steep cliff along the sea. Mast G is located at relatively low elevation and surrounded by mountains. The wind velocity was measured at these seven sites at eight different heights, which are 5, 10, 20, 35, 50, 75, 100 and 150 mm above the surface of the terrain model, corresponding to 10, 20, 40, 70, 100, 150, 200 and 300 m in the real scale.

2.2. Flow measurement

For the measurement of turbulent flow in complex terrain, the X-wire probes have been widely used. However, as pointed out by Ishihara et al. [5], the X-wire measurement cannot give reasonable accuracy in the wake region where the reverse

flow exists and the split-fiber probe was recommended. Actually, the X-wire measurement becomes inaccurate because of not only the existence of the reverse flow but also the strong across wind. This is because the X-wire measurement is based on following two assumptions: (1) the longitudinal component of the wind velocity is positive; and (2) the cross wind components is smaller than the longitudinal component. However, the flow in complex terrain can violate these assumptions.

In this study, measurements were made using constant temperature hot-wire anemometer (Kanomax 1010) with both X-wire (Kanomax 0249R-T5) and split-fiber (Kanomax 1288) probes to clarify the problem of the X-wire probe. Sensors were calibrated as described by Ishihara et al. [5]. The analog voltage was low-pass filtered in 500 Hz and digitized in a sampling rate of 1 kHz. A sampling time of 20 s was used for the mean velocities and the turbulence statistics.

3. Experimental results and discussion

Although the experimental results for all the sites are different, some sites show similar features. Thus, four representative sites, that is, sites A, B, F and G, are chosen and the surrounding terrain around the sites are shown in Fig. 3. In the following section real scale will be used.

3.1. The X-wire and the split-fiber probe measurements

Although the X-wire probes have been widely used for the measurement in complex terrain, they may contain large errors. Two examples are given in Fig. 4.

Fig. 4a shows the vertical profile of longitudinal wind velocity at the site B with the southwesterly wind. The X-wire measurement overestimates the mean wind speed
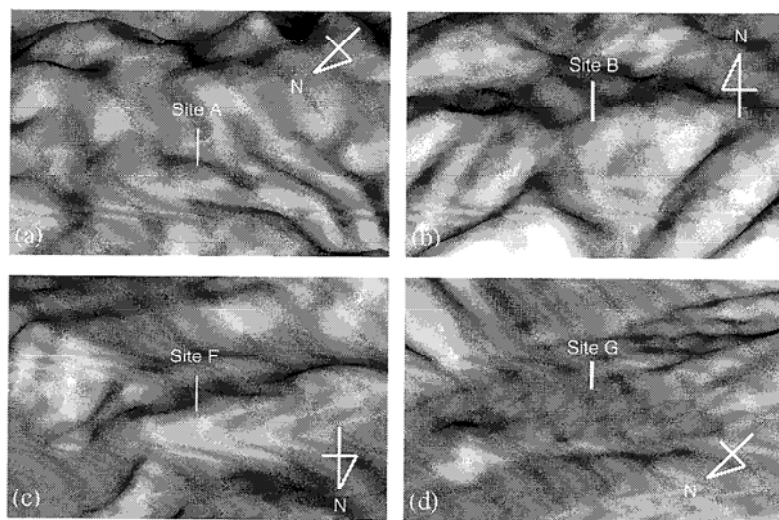

Fig. 3. The surrounding terrain of representative measurement sites.
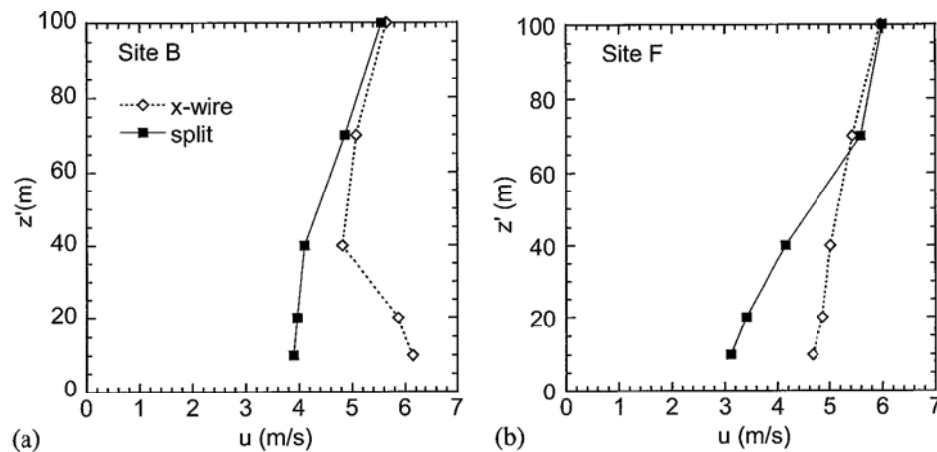
Fig. 4. The vertical profile of the longitudinal wind velocity measured by the X-wire probe and the split-fiber probe: (a) at site B with southwesterly wind; and (b) at site F with the northeasterly wind.

near the surface. There is a valley to the south of the site as shown in Fig. 3b. When the wind is southwesterly, the wind direction may be forced to change by this valley and the transverse component of the wind velocity may become quite large.

As mentioned above, the measurement by the X-wire probe may be inaccurate when the flow separates. Fig. 4b shows the vertical profile of longitudinal wind velocity at site F with the northeasterly wind. The overestimation by the X-wire probe is remarkable, since site F is located near the cliff (Fig. 3c) and the flow may separate at the edge when the wind is northeasterly. This may cause the error in the X-wire measurements.

The flow field around these sites will be described using the result of numerical simulation in Section 5.3. In the following section only the measurements by the split-fiber probe are discussed.

3.2. Mean field

Mean wind speed is the most important factor in engineering applications. The vertical profiles of the longitudinal component of the mean wind velocity at the four representative sites are shown in Fig. 5. The thick line shows the undisturbed flow and lines with symbols show the flow above the terrain. To investigate the topographic effect on the mean wind speed quantitatively, the topographic multiplier for wind speed is defined as U/U_0, where U denotes the wind speed above the terrain and U_0 represents that of undisturbed flow. The variations of the topographic multipliers with the wind direction at three typical heights are shown in Fig. 6.

At site A, the wind speed profiles and the topographic multipliers show relatively small variation with the wind direction (Figs. 5a and 6a) and the topographic multipliers exceed one for almost all the wind directions. This is because site A is surrounded by relatively flat terrain and located at a high elevation.

In contrast to site A, site B is surrounded by more complex terrain. The wind speed profiles and the topographic multipliers vary remarkably with the wind
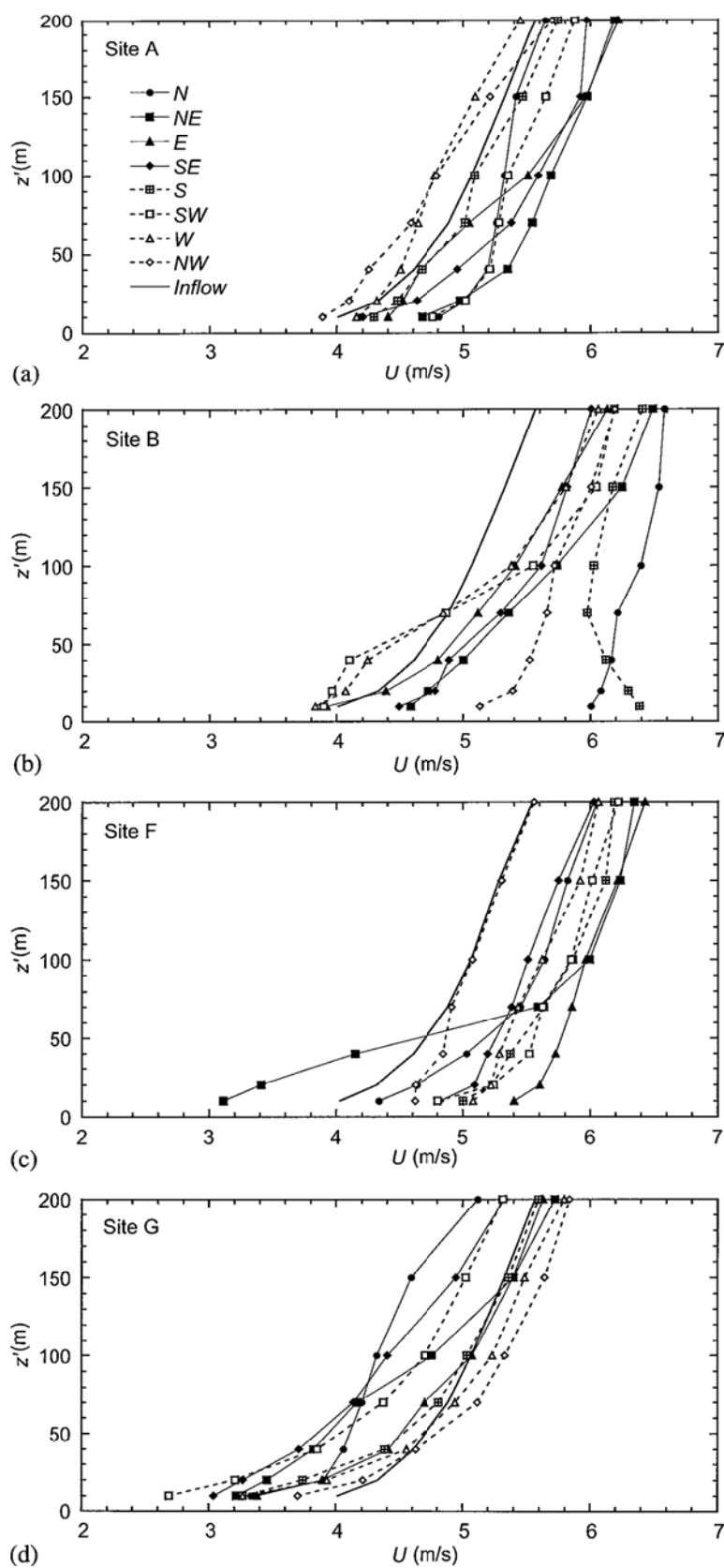
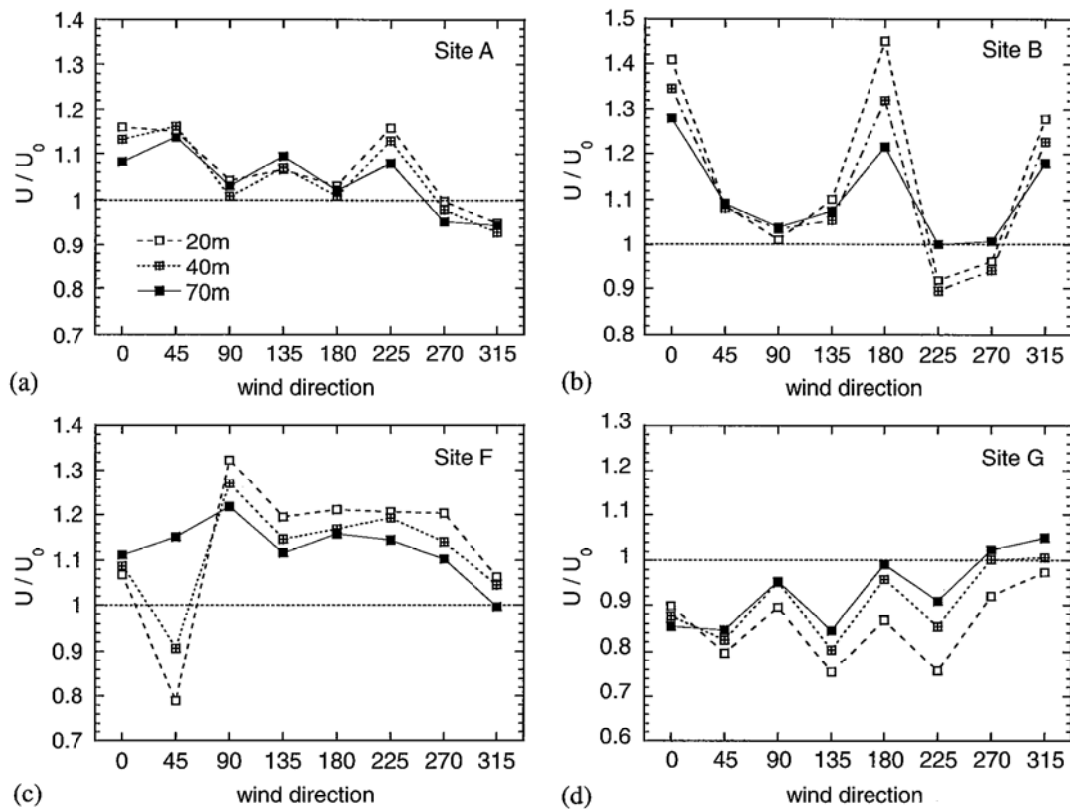Fig. 5. The vertical profiles of mean wind speed (U) at four representative sites.

Fig. 6. Topographic multipliers for wind speed at four representative sites.

directions. The topographic multiplier with the southwesterly wind reaches 1.45 at the height of 20 m and 1.22 at the height of 70 m (Fig. 6b). As shown in Fig. 3b, there is a valley to the south of site B, which causes the channeling effect and the increase in velocity with the southerly wind. In this wind direction, the wind speed near the surface is larger than that at the height of 70 m (Fig. 5b).

The most dramatic decrease of wind speed near the surface can be seen at site F with the northeasterly wind (Fig. 5c). The topographic multiplier with the north-easterly wind decreases to 0.79 at the height of 20 m while it is 1.15 at the height of 70 m (Fig. 6c). There is a cliff about 200 m away from site F as shown in Fig. 3c, and the flow may separate at the edge when the wind is northeasterly. This is the reason why the wind speed decreases with the northeasterly wind.

Since site G is located at relatively low elevation compared to the surrounding terrain, wind speed decreases in almost all the wind directions (Fig. 5d) and the topographic multiplier for the mean wind speed stays lower than 1.0 (Fig. 8d).

3.3. Turbulence field

Turbulence in complex terrain is also an important factor for the safety of structure. Standard deviation of the wind velocity is one of the most important turbulence statistics.

Fig. 7 shows the vertical profiles of the standard deviation of the longitudinal component of the wind velocity σ_u for the four representative sites. The topographic multiplier for the standard deviation is defined as σ_u/σ_{u0}, where σ_u denotes the standard deviation of the wind velocity above the terrain and σ_{u0} denotes that of the undisturbed flow. The variations of the topographic multiplier for the standard deviation with the wind direction at three heights are shown in Fig. 8.

At site A, the turbulence at the height of 200 m is as large as that near the surface with the northerly and westerly wind (Fig. 7a). This is because the terrain to the north and to the west of the site is very complex. At the lower levels, the topographic multipliers show relatively small variation with the wind direction (Fig. 8a).

The topographic multipliers at site B show larger variation with the wind direction (Fig. 8b). The maximum standard deviation can be found at the height of 70 m with the southwesterly wind (Fig. 7b). In this case, the wind direction rapidly changes near the surface and may generate the large turbulence as discussed in Section 5.3. On the other hand, the turbulence with the southerly wind is almost the same as the undisturbed flow although the wind speed increases due to the channeling effect.

At site F, large peak in the vertical profile can be seen in Fig. 7c. This is because of the flow separation as shown in Fig. 18. The topographic multiplier in this wind direction at the height of 40 m shows a large value of 2.7 while it is less than 1.5 in the other directions (Fig. 8c).

Since the surrounding terrain of site G is relatively flat, the turbulence does not increase much. The topographic multiplier stays almost constant except for the northeasterly and the northerly wind (Fig. 8d). The terrains to the northeast and to the north of the site are complex and the large turbulence may be generated by the upwind terrain. The maximum value of the turbulence appears at the height of 100 m in the northeasterly wind and 150 m in the northerly wind (Fig. 7d).

3.4. Applicability of the power law to the wind prediction over complex terrain

Due to the limitation of the height of the tower in the field observation, the wind speed at higher level has to be estimated from the lower level measurement. Power law is widely used to present the wind speed profile:

$$U(z) = U(z_1)\left(\frac{z}{z_1}\right)^{\alpha_U}, \tag{1}$$

where $U(z)$ is the mean wind speed at the height of z, z_1 is the reference height and α_U is a exponent, which is assumed to be a function of the location. When the wind speed at two lower levels are measured, α_U can be obtained by the power law and then the mean wind speed at any height can be estimated.

To verify the applicability of the power law to the wind prediction over complex terrain, mean wind speed at the height of 70 m is estimated from two different pairs of heights and compared with the measurement. In the first case, mean wind speeds
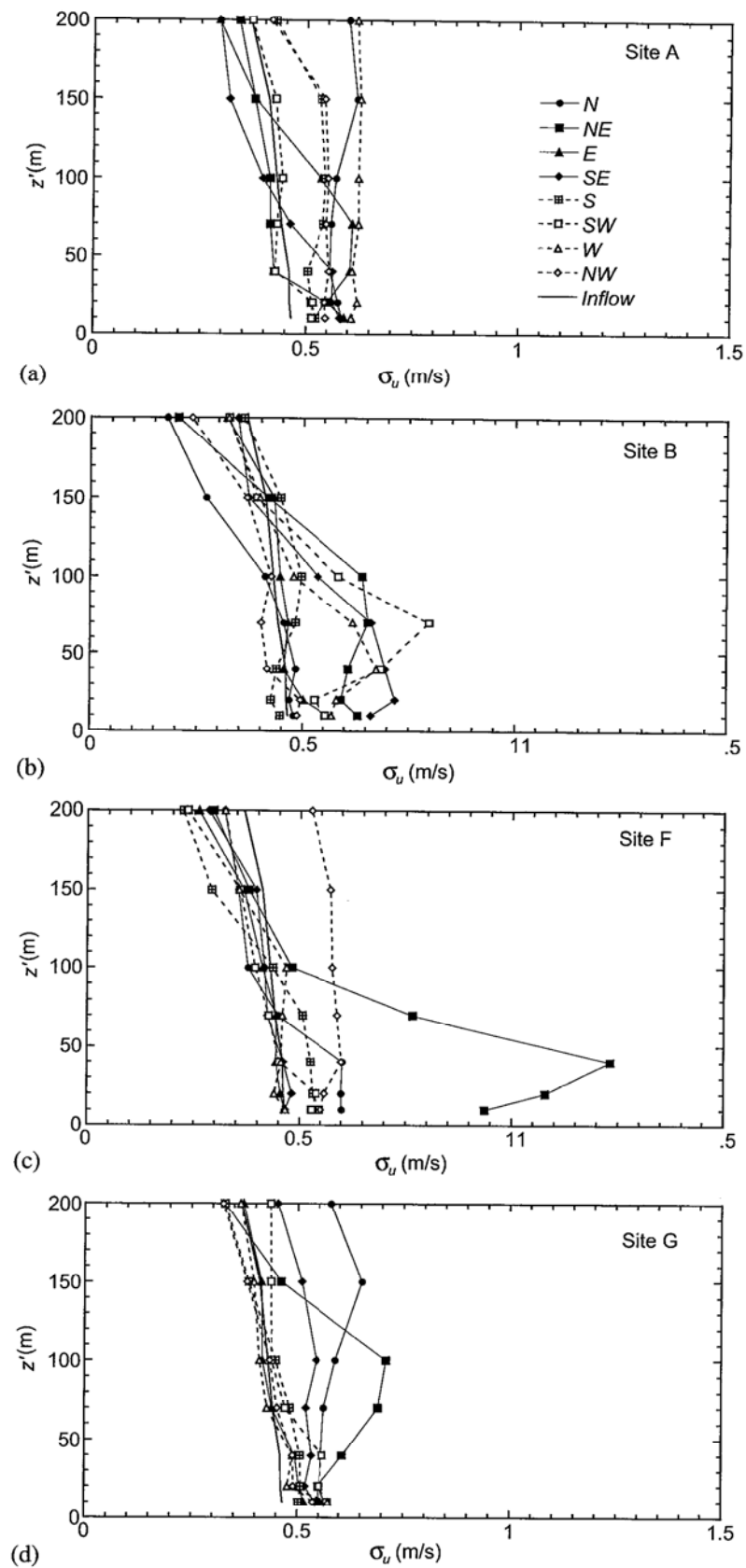
Fig. 7. The vertical profiles of the standard deviation of the longitudinal component of the mean wind velocity, σ_u, at four representative sites.
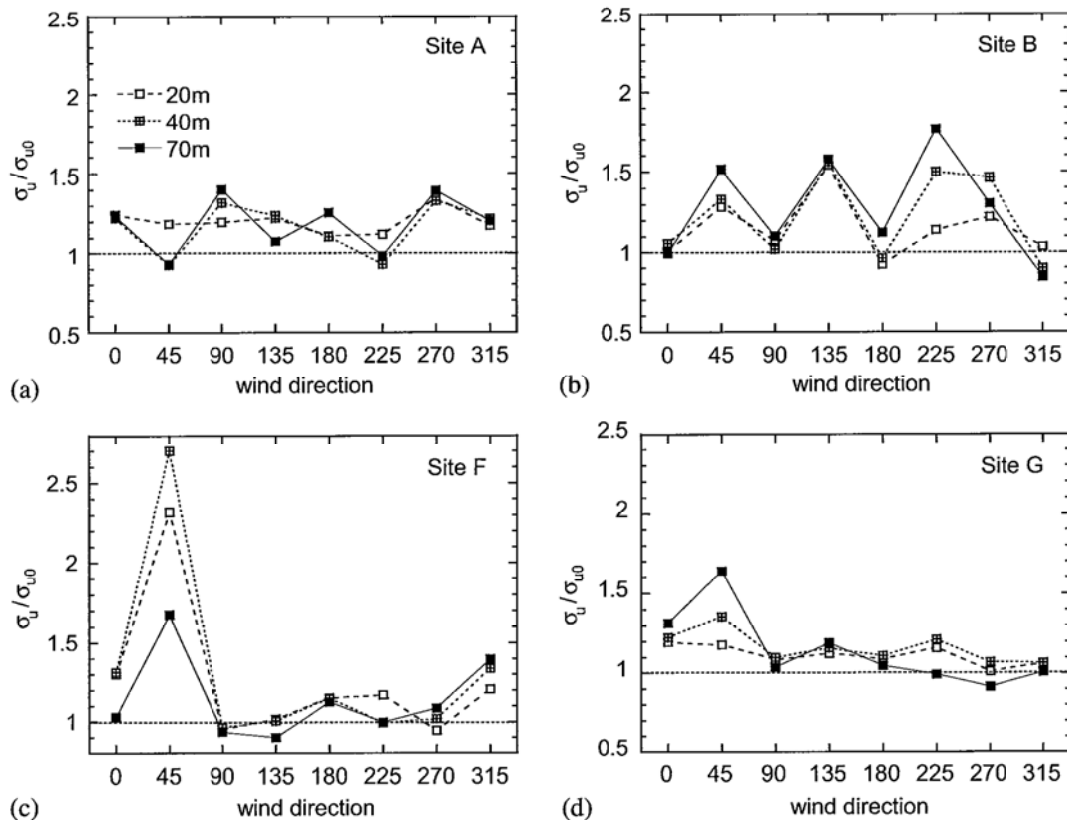
Fig. 8. Topographic multiplier for the standard deviation of the wind velocity at four representative sites.

obtained at the height of 10 and 20 m are used and the measurements at 20 and 40 m are used in the other case.

Normalized error of the estimation, ε_U is defined as

$$\varepsilon_U = \frac{U_e - U_m}{U_0} \times 100, \qquad (2)$$

where U_e and U_m denote the estimated and measured wind speeds, respectively, and U_0 is the wind speed in the undisturbed boundary layer.

Fig. 9 shows the comparison of estimated and measured wind speeds at the height of 70 m at the four representative sites for all the wind directions. In case of the estimation from the height of 10 and 20 m, some points are located far from the diagonal line (Fig. 9a). The maximum error can be found at site F with the northeasterly wind, where the estimated wind speed is 4.0 m/s while the measured wind speed is 5.6 m/s. This implies the normalized estimation error of 33%. The root mean square of the normalized error for all the sites and wind directions is 8.7%. Although the estimation from the wind speed at the height of 20 and 40 m shows more reasonable results for most sites and directions (Fig. 9b), the errors in some sites are even large. The maximum error of 15% can be seen at site F with the northeasterly wind. The root mean square of the normalized error is 4.7% in this case.
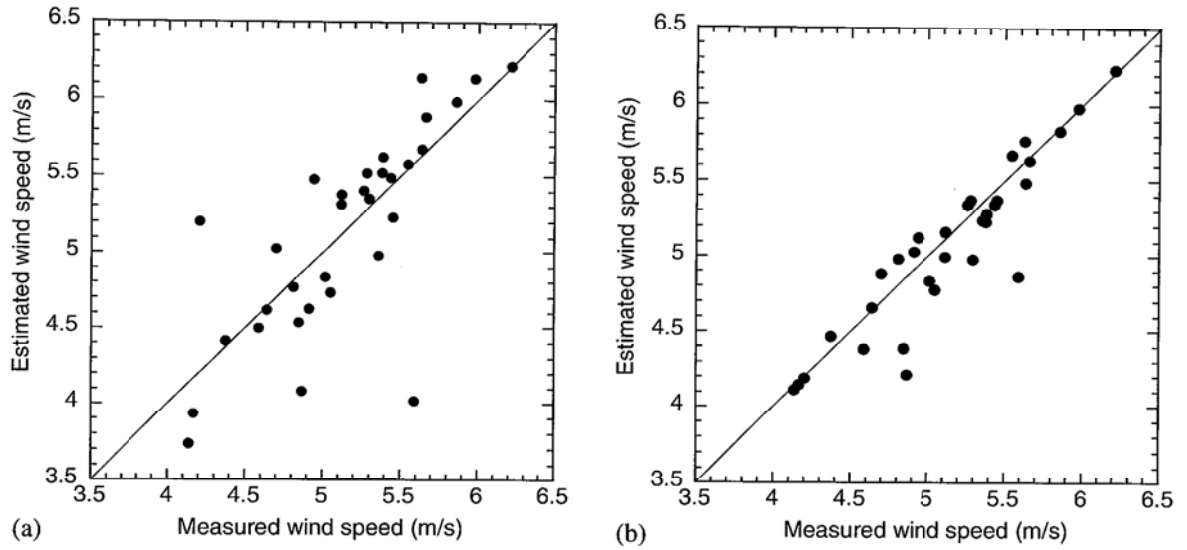
Fig. 9. Comparison of measured and estimated mean wind speeds at the height of 70 m by the power law: (a) estimation from the height of 10 and 20 m; and (b) from 20 and 40 m.

Estimation of turbulence is also important. Turbulence intensity, I, is defined as a ratio of standard deviation to mean wind speed. For the estimation of turbulence intensity at higher levels, power law can also be used [6]. The power law for the turbulence intensity is described as

$$I(z) = I(z_1)\left(\frac{z}{z_1}\right)^{\alpha_I}, \tag{3}$$

where $I(z)$ is the turbulence intensity at the height of z, α_I is the exponent. The difference between estimated and measured turbulence intensities δ_I is defined as

$$\delta_I = I_e - I_m, \tag{4}$$

where I_e and I_m denote the estimated and measured turbulence intensities, respectively.

Turbulence intensities at the height of 70 m estimated from the measurement at the height of 10 and 20 m, and from 20 and 40 m are shown in Fig. 10. At site F with the northeasterly wind, the difference shows the maximum value of 21% points for both the estimations. The root mean square of the difference is 4.1% points for the estimation from the height of 10 and 20 m, and 4.3% points from 20 and 40 m.

These results indicate that the power law cannot give accurate estimations for the mean wind speed or the turbulence intensity in complex terrain.

4. Numerical simulation

An advantage of the numerical simulation to the wind tunnel test is that the whole flow field can be visualized. Wind flow over the sites obtained by the non-linear
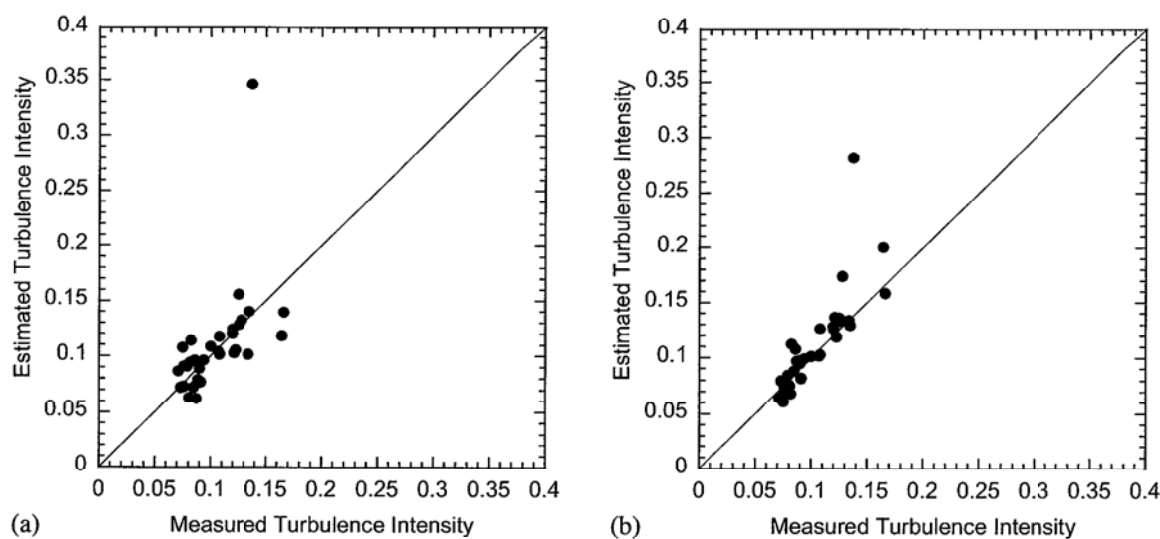
Fig. 10. Comparison of measured and estimated turbulence intensities at the height of 70 m by power law: (a) estimation from the height of 10 and 20 m; and (b) from 20 and 40 m.

model and the linear model will be revealed and the performance of the models will be examined.

4.1. Numerical model and boundary conditions

The non-linear wind prediction model developed by the authors [7] is used in this study. Reyolds averaged Navier–Stokes equation is used as governing equations and the standard k–ε model [8] is adopted to estimate the turbulence. Because of the necessity of resolving the complex terrain, the arbitrary non-orthogonal collocated grid system is used. As a surface boundary condition, the shear stress calculated by the log law is considered as a drag term in the momentum equations for the surface adjacent cells. The detail of the numerical model and the boundary conditions are described by Ishihara and Hibi [7]. The measured velocity and turbulence at 6 m upstream to the turn table center are used as an inlet boundary condition in the numerical simulation.

As a conventional linear model, LINCOM [9] based on the model proposed by Jackson and Hunt [1] was used. The linear model looses its prediction accuracy when the slope angle is large. LINCOM contains the model to calculate the turbulence, but the turbulence model also has the limitation of the slope angle [9].

4.2. Estimation of normal Reynolds stresses based on the k–ε model

In the non-linear model described above, mean wind velocity and the turbulent kinetic energy k are explicitly predicted but the normal Reynolds stresses are not. If the turbulence structure is isotropic, they can be estimated by the standard k–ε

model. However, because the turbulence structure is anisotropic in the boundary layer, the method proposed by Paterson and Holmes [10] will be used.

In the turbulent boundary layer, there is a relation among the standard deviations of each velocity component as

$$\sigma_u : \sigma_v : \sigma_w = 1 : 0.68 : 0.45. \tag{5}$$

Then, normal Reynolds stresses can be expressed in terms of k as

$$\overline{u'^2} = 1.2k, \quad \overline{v'^2} = 0.56k, \quad \overline{w'^2} = 0.24k. \tag{6}$$

These relations will be used to predict the normal Reynolds stresses in complex terrain.

5. Numerical results and discussion

5.1. Flow in the undisturbed boundary layer

To verify the accuracy of the non-linear model and the inlet boundary conditions described above, flow in the undisturbed boundary layer was predicted and compared with the measurements. The vertical profiles of the mean wind speed and the standard deviation in the undisturbed boundary layer are shown in Figs. 11 and 12. The numerical results show fairy good agreement with the measurements. These results will be used to calculate topographic multipliers for the mean wind speed and standard deviation.

5.2. Flow over complex terrain

As mentioned in Sections 3.2 and 3.3, the wind flow changes remarkably with the wind direction at sites B and F. The topographic multipliers for the mean wind speed and for the standard deviation will be investigated by the linear and the non-linear models.
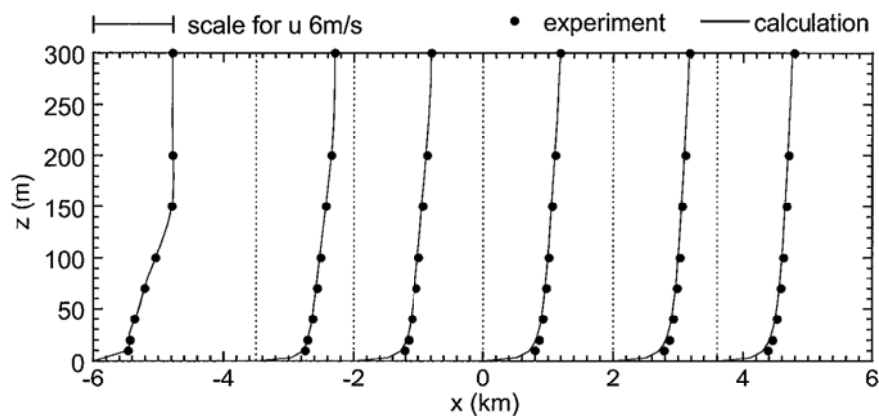
Fig. 11. The vertical profiles of mean wind speed in the undisturbed boundary layer.
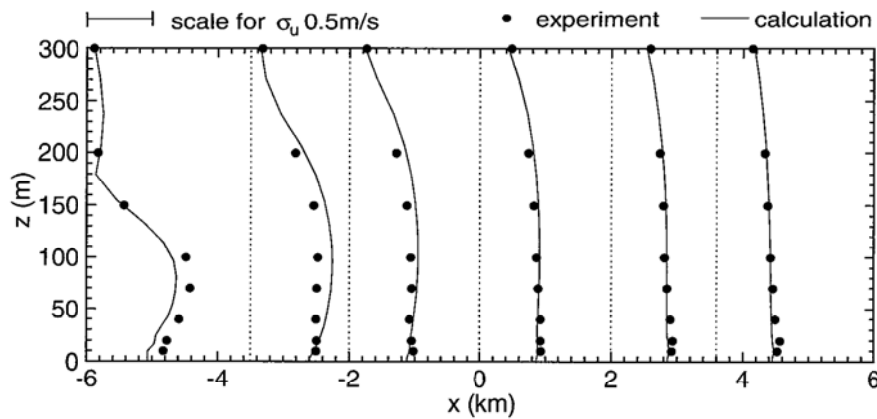
Fig. 12. The vertical profiles of the standard deviation of the wind velocity in the undisturbed boundary layer.
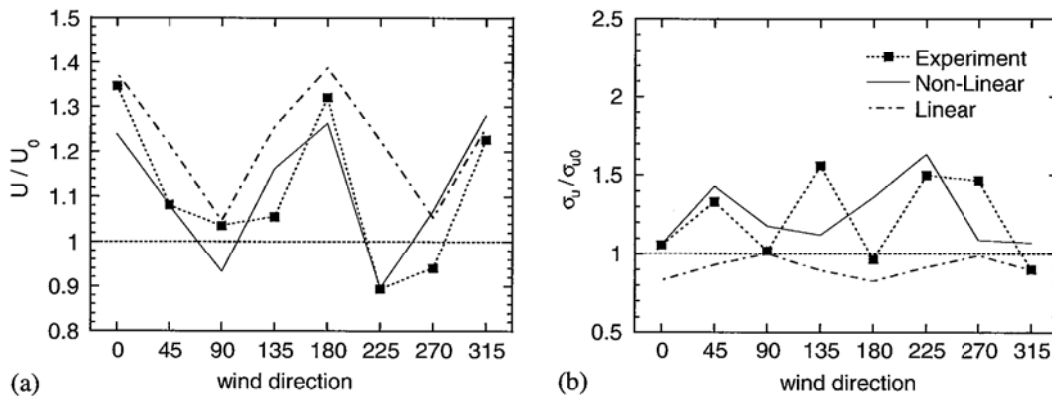

Fig. 13. Measured and predicted topographic multipliers at site B: (a) for the mean wind speed; and (b) for the standard deviation.

Fig. 13a shows variation of the topographic multiplier for the mean wind speed with the wind direction at the height of 40 m at site B. Flow is strongly influenced by the surrounding terrain and the topographic multiplier varies considerably with the wind direction. The non-linear model can predict this feature and gives fairly good agreement with the experiment, while the linear model overestimates the wind speed with the southwesterly wind (225°). This error is due to the inability of the linear model for predicting the rapid change in the wind direction, which will be shown in Fig. 16. The topographic multiplier for the standard deviation is shown in Fig. 13b. It also varies with the wind direction. This feature is caught by the non-linear model while the result by the linear model largely underestimates the turbulence.

Site F is characterized by the flow separation at the edge of the cliff. When the wind is northeasterly, remarkable decrease in the mean wind speed can be seen in Fig. 14a. The non-linear model can predict this wind speed decrease with the northeasterly wind while the linear model overestimates the mean wind speed. The non-linear model can also predict the increase in the turbulence (Fig. 14b) with
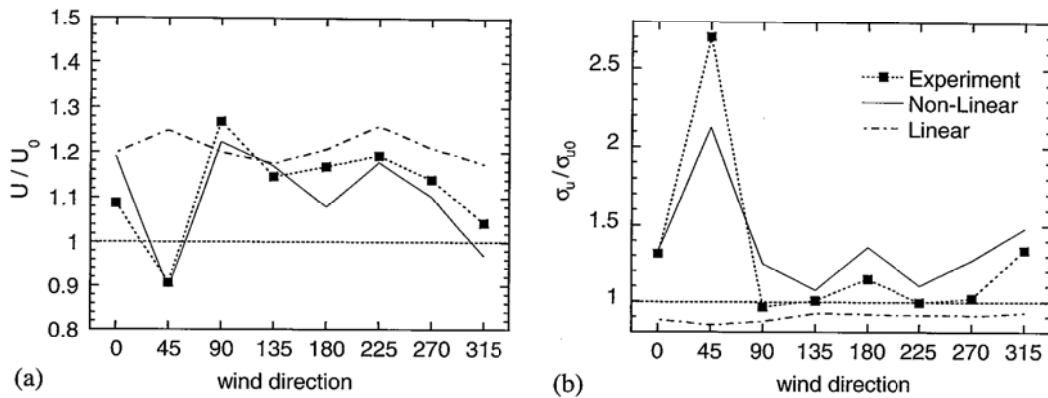
Fig. 14. Measured and predicted topographic multipliers at site F: (a) for the mean wind speed; and (b) for the standard deviation.

the northeasterly wind while the linear model largely underestimates the turbulence. This is because the linear model cannot predict the flow separation.

5.3. The error in the X-wire measurement

The X-wire measurement contains some errors as mentioned in Section 3.1. The reason of the error will be discussed and explained using the numerical result by the non-linear model.

Fig. 15 shows the vertical profile of mean wind speed at site B with the southwesterly wind. The value measured by the split-fiber probe is consistent with the prediction while that by the X-wire probe is much larger especially near the terrain surface. The mean wind velocity vector around the site is shown in Fig. 16. The wind direction is forced to change to southerly by the local valley. This causes increase in the transverse component of the wind velocity. This is the reason why the X-wire measurement gives a different profile near the terrain surface.

The existence of the reverse flow can also be the reason of the error. Fig. 17 shows the vertical profile of mean wind speed at site SF2 with the northeasterly wind, which is located at the windward of site F (Fig. 18). The overestimation by the X-wire probe can also be seen. Fig. 18 shows the mean velocity vector in the vertical cross section around the site. The flow separates at the edge of the cliff and reverse flow can be observed near the terrain surface. This is the reason why the X-wire measurement overestimates the wind speed.

6. Conclusion

The characteristics of the wind flow in a complex terrain are investigated by wind tunnel test using X-wire and split-fiber probes. Numerical simulations by the linear
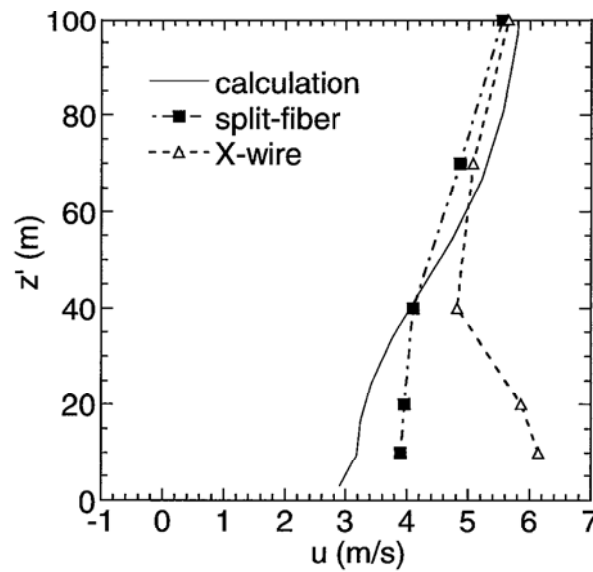
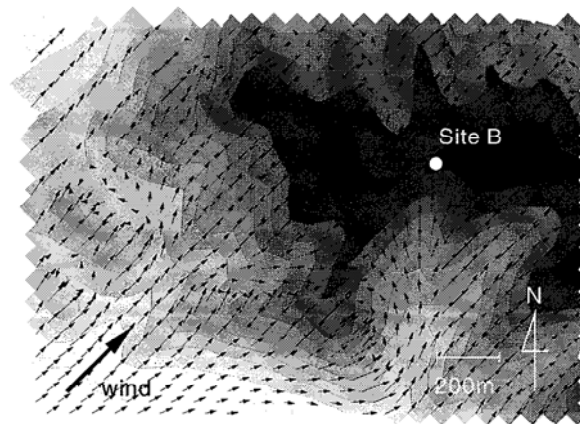Fig. 15. The vertical profile of mean wind speed at site B with the southwesterly wind.

Fig. 16. Mean wind velocity vector around site B with the southwesterly wind.

and the non-linear model are carried out to examine the performance of the models. The following summarizes the major conclusions of this study:

(1) The split-fiber probe can give a reasonable accuracy while the conventional X-wire probe measurement contains a large error because of the existence of reverse flow and strong across wind in complex terrain.

(2) Local wind in complex terrain is very complex. Wind speed decreases remarkably behind the cliff because of the flow separation and in the depression area due to the sheltering effect. Remarkable change in the wind direction and wind increase are observed around the valley due to the channeling effect.

(3) Above complex terrain, it is difficult to apply the power law to estimate the wind speed or the turbulence intensity at the higher level from the measurements at lower levels.
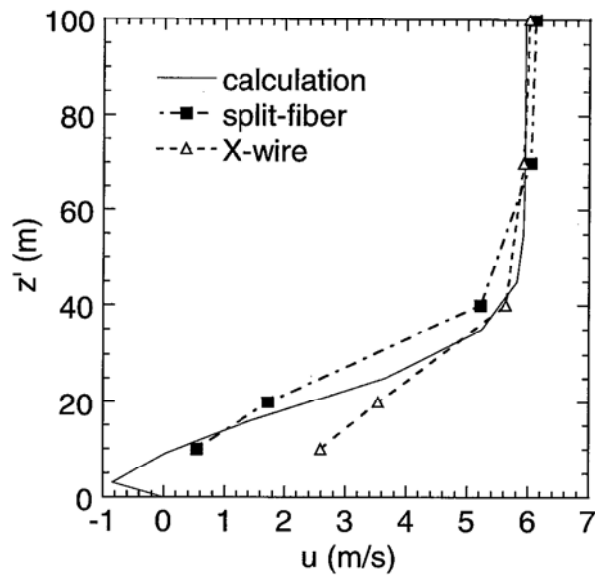
Fig. 17. The vertical profile of mean wind speed at site SF2 with the northeasterly wind.
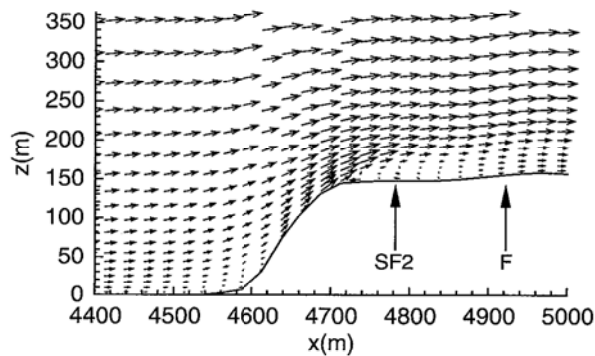

Fig. 18. The cross section of the terrain and the mean velocity vector around site SF2.

(4) The non-linear model gives fairly good agreement with the measurements. On the other hand, the linear model overestimates the mean wind speed and underestimates the turbulence since it cannot predict the flow separation nor the large change in the wind direction.

References

[1] P.S. Jackson, J.C.R. Hunt, Turbulent wind flow over a low hill, Q. J. R. Meteorol. Soc. 101 (1975) 929–955.
[2] P.J. Coelho, J.C.F. Pereira, Finite volume computation of the turbulent flow over a hill employing 2d or 3d non-orthogonal collocated grid systems, Int. J. Numer. Methods Fluids 14 (1992) 423–441.
[3] A. Maurizi, J.M.L.M. Palma, F.A. Castro, Numerical simulation of the atmospheric flow in a mountanious region of the north of portugal, J. Wind Eng. Ind. Aerodyn. 74–76 (1998) 219–228.
[4] NEDO, Evaluation of the wind resource prediction models, 1998 (in Japanese).

[5] T. Ishihara, K. Hibi, S. Oikawa, A wind tunnel study of turbulent flow over a three-dimensional steep hill, J. Wind Eng. Ind. Aerodyn. 83 (1999) 95–107.

[6] T. Ishihara, M. Matsui, K. Hibi, Characteristics of the vertical wind profile in neutrally atmospheric boundary layers, part 1: strong winds during non-typhoon climates, J. Wind Eng. 65 (1995) 1–15 (in Japanese).

[7] T. Ishihara, K. Hibi, Numerical study of turbulent wake flow behind a three-dimensional steep hill, Wind Struct. 5 (2002) 317–328.

[8] W.P. Jones, B.E. Launder, The prediction of laminarization with a two-equation model of turbulence, Int. J. Heat Mass Transfer 15 (1972) 301–314.

[9] J.M. Santabárbara, T. Mikkelsen, R. Kamada, G. Lai, A.M. Sempreviva, Lincom. wind flow model, Risø National Laboratory, Denmark, 1994.

[10] D.A. Paterson, J.D. Holmes, Computation of wind flow over topography, J. Wind Eng. Ind. Aerodyn. 46 & 47 (1993) 471–476.